Effect of interfacial transition zone and aggregates on the time-dependent behavior of mortar and concrete

Farid Benboudjema, Emmanuel Guillon, Jean Michel Torrenti

Effect of interfacial transition zone and aggregates on the time-dependent behavior of mortar and concrete

F. Benboudjema & E. Guillon
Laboratoire de Mécanique et Technologie, ENS Cachan, Cachan, France.

J.-M. Torrenti
Institut de Radioprotection et de Sûreté Nucléaire,Fontenay-aux-Roses, France.

ABSTRACT: Concrete has a high degree of heterogeneity. About 75 % of the volume is occupied by aggregates. Even if most properties of concrete come from the cement paste (shrinkage, creep …), aggregates modify in a large extent the properties of concrete. In this paper, the effect of sand grains, on the cracking process of mortars, is numerically studied. Digital picture of mortar are used for finite element simulations to study the drying shrinkage. The obtained cracking pattern is compared to the observed one in the literature, which shows good agreements.

Keywords: instructions, paper preparation, format, submission deadline

1 INTRODUCTION

Durability and long-time serviceability of concrete structures, like containment vessels of nuclear power plants, are greatly affected by time-dependent strains. Indeed, creep and shrinkage cause cracking, losses of pre-stress and redistribution of stresses.

Cracking may be due to different mechanisms. Non-homogeneous drying induces a gradient of shrinkage strain. Indeed, inner parts of the material shrink slower than the skin, resulting in tensile stresses in the skin. Therefore, cracking may occur if tensile stresses overcome tensile strength. Besides this type of restraint, the composite character of cement based materials contributes to cracking. Indeed, concrete is a highly heterogeneous material. On the macroscale, large aggregates are bonded by a mortar matrix. On the mesoscale, the mortar matrix is constituted of small aggregates and sand bonded by cement paste. On the microscale, the cement paste includes pores (fully or partially saturated voids) and different hydrous (C-S-H, portlandite and ettringite mainly) and anhydrous constituents. Since time-dependent strains occur only in the cement paste, radial and circumferential cracking occurs around the aggregate particles (Goltermann 1995). Furthermore, the heterogeneous aspect of cement-based materials is amplified by the presence of an Interfacial Transition Zone (ITZ) between the cement paste and sand (and aggregates).

The ITZ can have an important effect on the properties of concrete. For instance, its relative stiffness and strength, with respect to the cement paste and/or aggregate ones, and its thickness affect the cracking and the mechanical properties of concrete. They are decisive in governing whether a crack should grow around an aggregate particle, or rather, would follow a path through the grain (van Mier & Vervuurt 1999). Moreover, more important the thickness of ITZ is, more degraded the mechanical properties of concrete are (Katz et al. 1999). These features may explain experimental evidences which show that higher value of aggregates stiffness does not lead to higher value of concrete stiffness (Sengul et al. 2002).

The importance of aggregate restraint on time-dependent deformation is poorly known (Bisshop & van Mier 2002). Indeed, most of numerical models for shrinkage and creep treat the mortar or concrete as a homogeneous material (Wittmann & Roelfstra 1980, Kim and Lee 1998, Bažant 2001 for instance). Moreover, a few attempts to relate time-dependent strains to composition of mortar or concrete by some rational calculations have been made (Nielsen & Monteiro 1993, Granger & Bažant 1995, Nielsen et al. 1995, Li et al. 1999). These calculations use homogenization techniques and time-dependent strains are treated by the

effective modulus method, which reduces the problem to quasi-elastic analysis. Furthermore, they assume concrete or mortars as a two or three phase materials, which do not take into account easily the size distribution or the shape of the aggregate particles. Moreover, these models can not take into account cracking of the cement paste, which can occur during drying or because of the restraint effect of aggregates.

In order to overcome this issue, finite element calculations can be performed, if an adequate mesh is generated. In this case, more complex and accurate models for the cement paste can be adopted. This approach has been previously used to study the drying process and the fracture process of concrete submitted to static or dynamic loadings (Roelfstra et al. 1985, Tijssens et al. 2001, Ciancio et al. 2003). In these two last approaches, the cracking of cement paste and ITZ is taken into account by the use of cohesive surfaces, which relate the tension transmitted over the contact surface to the relative displacement between the surfaces. However, the effects of drying on cracking do not seem to have been studied yet.

The objective of this paper is to study numerically the effect of sand particles on the drying shrinkage of mortars. The material models for each phase of concrete as well as the generation of the meso-structure are first presented in section 2 (meso-modeling). Then, numerical simulations are performed in section 3 to illustrate the adopted approach. Finally, the main conclusions and some perspectives are summarized in section 4.

2 MODELING OF THE MORTAR BEHAVIOR

In this study, mortar is assumed to be a three-phase composite material constituted of sand, cement paste and ITZ.

In this paper, the structure of the mortar, at the mesoscale, is taken into account explicitly by using a finite element mesh of the heterogeneous material. We use an available algorithm used for cement hydration (CEMHYD3D, Bentz, 1997) to generate a three-dimensional mortar meso-structure (100×100×100 pixels). We consider at the beginning two phases: cement paste and sand particles. In order to obtain the desired (three-dimensional) particles size distribution of sand, spherical particles (content and diameter) are added successively. Since the volume percentage of sand is great, the numerical generation of the meso-structure may be difficult. Therefore, largest particles are first placed randomly in the material. Then, the generated microstructure picture is modified by a developed program in order to place the ITZ as an interface element at the cement paste/sand particles interface. Finally, the geometry is converted into a readable format by a available Finite Element Code (Cast3m). A finite element mesh, unveiling each phase, is given in Figure 1.

Each phase has its specific behavior, which is given below.

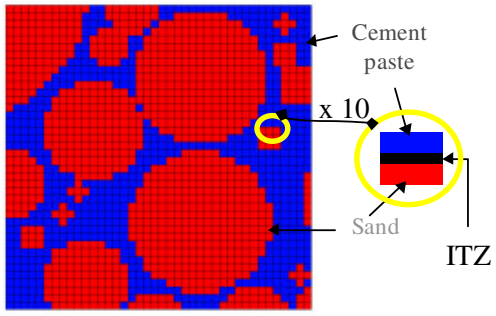

Figure 1. Finite element mesh of a mortar.

2.1 *Sand behavior*

Sand particles are assumed to be elastic:

$$\boldsymbol{\varepsilon} = \frac{1+\nu_g}{E_g}\boldsymbol{\sigma} - \frac{\nu_g}{E_g} tr\boldsymbol{\sigma}\mathbf{I} \qquad (1)$$

where E_g and ν_g are the sand Young's modulus and Poisson's ratio, which are taken equal to 34 GPa and 0.2, respectively. $\mathbf{I}$ is the second order unit tensor.

Therefore, sand particles do not fracture and restrain creep and drying shrinkage of the cement paste. Moreover, they slow down the drying process.

2.2 *Cement paste behavior*

The cement paste is assumed to be a visco-elasto-plastic damage material (Benboudjema 2002). The numerical model is based on the theory of non-saturated porous media and the effective stress concept. It allows for obtaining an original model based on physical concept. The adopted models are briefly presented below.

2.2.1 *Drying*

The drying of concrete is modeled here by a diffusion-type equation, i.e. second Fick's law:

$$\dot{C} = \nabla\left(D\left(C\right)\nabla C\right) \qquad (2)$$

in which C is the water content; and D is the apparent diffusivity, which varies in a strongly non-linear manner as a function of the water content. The dot represents the derivative with respect to time.

The diffusivity is calculated with the relationship derived by Xi et al. (1994). The relative humidity is relied on the water content by the desorption isotherm curve. The BSB model (Xi et al. 1994), called also the three-parameter BET model, is used here to calculate the desorption isotherm curve

2.2.2 *Cracking*

The behavior of cracked concrete is modeled by a damage model coupled with softening plasticity, developed by the authors (Benboudjema et al. 2001). The plastic strain describes the irreversible deformation observed experimentally after unloading. The accompanying stiffness degradation due to microcracks is given by the second order damage tensor **D**.

The nominal stresses σ are related to the effective stresses $\tilde{\sigma}$, which act on the uncracked material only, by the following relationship:

$$\boldsymbol{\sigma} = \left(\mathbf{I} - \mathbf{D}\right) \cdot \tilde{\boldsymbol{\sigma}} \tag{3}$$

Effective stresses are related to the elastic strain by:

$$\tilde{\boldsymbol{\sigma}} = \mathbf{E}^{\mathbf{0}} \cdot \boldsymbol{\varepsilon}^{e} \tag{4}$$

where $\mathbf{E}^{\mathbf{0}}$ is the second order elastic stiffness tensor of the cement paste.

The damage process is assumed here to be orthotropic in tension, where orthotropy is induced by cracking. Hence, a tensorial damage variable is considered. Damage evolution is related to the cumulative plastic strains. As a matter of fact, experimental evidences show that this choice is relevant for concrete (Ju 1989). The evolution function is of exponential type (Lee & Fenves 1998).

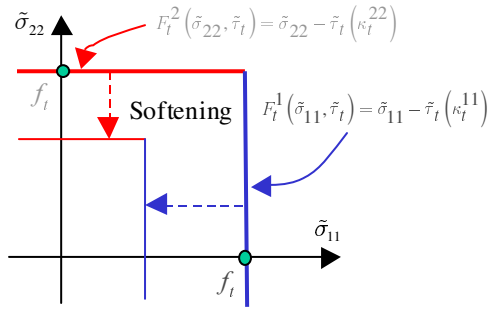

Figure 2. Rankine criteria in plane stresses conditions.

The coupling between damage and plasticity is based on the effective stress concept and on the hypothesis that the undamaged material behavior is elasto-plastic (Ju 1989). In order to reproduce a suitable behavior in tension, three independent Rankine criteria in tension are used (Fig. 2). This allows for retrieving an orthotropic behavior.

The Rankine criteria are written as:

$$F_t^i\left(\tilde{\sigma}, \boldsymbol{\kappa}_t\right) = \tilde{\sigma}_{ii} - \tilde{\tau}_t^i\left(\kappa_t^{ii}\right) \tag{5}$$

where τ_t is the nominal strength in tension and κ_t^{ii} is the i^{th} principal tensile cumulative plastic strain. Then, the plastic strain rate is obtained by Koiter assumption.

Strain softening induces inherent mesh dependency and produces failure without energy dissipation (Bažant 1976). In order to avoid these features, the fracture energy approach, proposed by Hillerborg et al. (1976) is used. The fracture energy density g_{ft} is related to fracture energy G_{ft} by a characteristic length l_e:

$$g_{ft} = \frac{G_{ft}}{l_e} \tag{6}$$

The characteristic length le is related to the size of the finite element (Feenstra 1993):

$$l_e = k_e \sqrt{A} \tag{7}$$

where k_e is a coefficient which depends upon the type of finite element and A is the area of the finite element (Feenstra 1993).

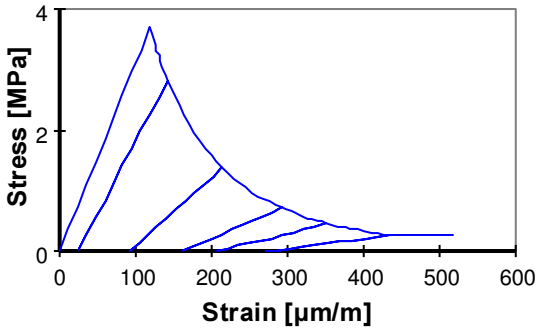

Figure 3. Stress-strain relationship in tension for the cement paste.

A typical curve for the stress-strain relationship is given in Figure 3. It is used in this study for the cement paste. The values of the mechanical parameters for the cement paste are given in Table 1.

Table 1. Mechanical parameters for the cement paste.

E [GPa]	ν	f_t [MPa]	g_{fi} [N.m^{-1}]
20	0.2	3.7	70

2.2.3 *Creep*

During drying process, self-equilibrated stresses are generated within the material. Therefore, the creep of concrete relaxes the induced stresses and reduces drying microcracking in the cement paste.

In this paper, a multiaxial model developed by the authors is used (Benboudjema et al. 2001), where the role of water is integrated in an original manner. In this model, the basic creep is considered to be the result of mechanisms, which are relevant compared to experimental findings (Benboudjema et al. 2001).

For constant stresses and a constant relative humidity h, the basic creep strains ε_{bc} can be expressed as:

$$\boldsymbol{\varepsilon}_{bc}(t) = h\,\mathbf{J}_{bc}(t)\cdot\tilde{\boldsymbol{\sigma}} \tag{8}$$

where $\mathbf{J}_{bc}$ is the basic creep compliance tensor, which depends upon material parameters (Benboudjema et al. 2001, Benboudjema 2002).

2.2.4 *Drying shrinkage*

Concrete is a material which is strongly hydrophilic and has an important specific surface. Indeed, its behavior is very sensitive to the hygrometric conditions.

The modeling of drying shrinkage is based on the mechanisms of disjoining pressure and capillary pressure, which seem to be predominant in the range 50 – 100 % of relative humidity (Soroka 1979). It is considered that drying shrinkage results from the elastic and the creep response of the solid skeleton under capillary pressure and disjoining pressure.

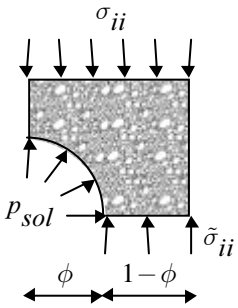

Figure 4. Effective stress concept (without cracking).

The pressure applied to the solid skeleton results from an average of the capillary pressure and the disjoining pressure. These effects are taken into account by the saturation degree S_l and a homogenized coefficient α_{rd} (equal to 1.49):

$$p_{sol} = \alpha_{rd} S_l\, p_c \tag{9}$$

where p_c is the capillary pressure. The coefficient α_{rd} can be identified from a drying shrinkage test.

The evolution of free drying shrinkage is derived directly from the framework of the mechanics of unsaturated porous media, using the concept of effective stress. Indeed, effective stresses $\tilde{\boldsymbol{\sigma}}$ are related to the apparent stresses $\boldsymbol{\sigma}$, the pore pressure p_{sol}, and the porosity ϕ by the following relationship (Fig. 4):

$$\boldsymbol{\sigma} = (1-\phi)\tilde{\boldsymbol{\sigma}} - \phi\, p_{sol}\mathbf{I} \tag{10}$$

2.3 *ITZ behavior*

The ITZ is modeled by zero-thickness interface elements between the cement paste and the sand particles. It is assumed that its behavior is elastic in compression, perfectly brittle in tension and plastic in shearing. The Mohr-Coulomb criterion has also been used.

For such elements, stress-strain relationship is replaced by a relation giving the stress σ transmitted over the contact surface to the relative displacement δu between the surfaces (Fig. 5).

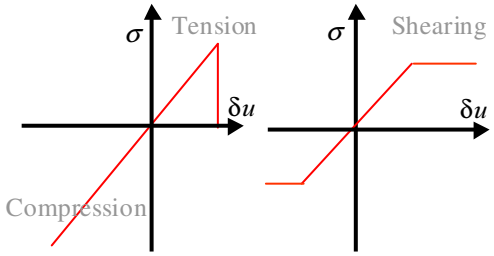

Figure 5. Behavior of the ITZ in compression, tension and shearing.

The values of the mechanical parameters for the ITZ are given in Table 2.

Table 2. Mechanical parameters for the ITZ.

E [GPa]	f_t [MPa]
10	1.85

3 NUMERICAL SIMULATIONS

Two numerical simulations were performed in order to illustrate our modeling approach. Firstly,

we study the fracture process of typical mortar under uniaxial tensile and compressive stresses. The cracks map is also compared to classical experimental observations. Then, drying shrinkage simulations are performed in order to study the effect of sand particles.

All calculations were performed under plane stresses conditions. The three-dimensional nature of cement composite seems to influence its fracture behavior (van Mier 1991). Moreover, the adopted algorithm for the generation of mortar allows only for controlling the volumetric concentration of sand particles. However, due to the limitations of computational resources, such calculations can not be achieved yet in a reasonable time. Furthermore, we choose to extract from the three-dimensional digital picture, a two-dimensional slice which has a similar concentration of sand particles.

Numerical simulations are carried out using a Finite Element Code (Cast3m).

3.1 *Instantaneous behavior simulations*

The fracture process of mortars is first studied, in tension and compression, in order to see whether our modeling is able to retrieve the principal experimental observations. A typical mortar is used, which corresponds to a "normalized mortar", according the French norm NF P 15-403. Its particles size distribution is given in Figure 6.

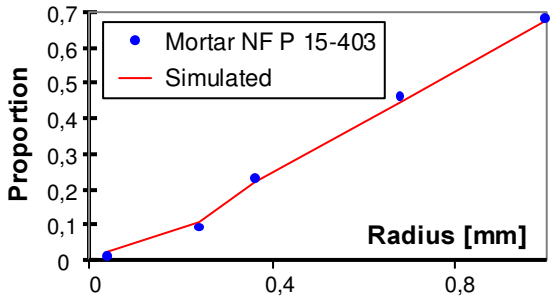

Figure 6. Cumulative sand concentration of the studied mortar ("normalized mortar" according to the French norm NF P 15-403): volumetric distribution of sand grains with respect to their radius.

A constant vertical displacement rate (positive in tension and negative in compression) at the top face of the specimen is applied. The horizontal displacement at the right face is free, but identical in all nodes. The other boundary conditions are given in Figure 7.

The numerical results are first presented for the tension test at the onset of failure. The damage fields in x and y-directions are displayed in Figure 8.

The magnified deformation of the specimen is presented in Figure 9.

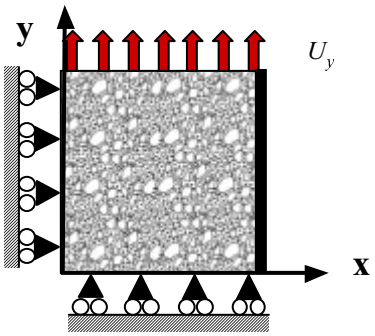

Figure 7. Illustration of the boundary conditions for the numerical simulations in tension and compression.

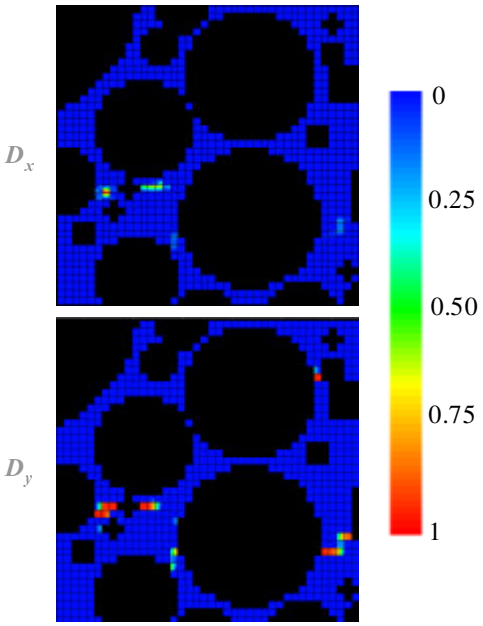

Figure 8. Damage fields (D_x and D_y variables) for the tension test.

In the tensile test, the damage is localized in few locations in the cement paste (Fig. 8). Moreover, the damage is preferentially oriented. There is less damage in the x-direction (vertical cracks) than in the y-direction (horizontal cracks).

Figure 9 shows that the development of fracture is highly governed by the presence of the weak ITZ, between sand grains and the cement matrix. Indeed the length of the damaged zone in the cement paste (Figure 8) is less than the one at the interface

cement paste/paste (Figure 9). Therefore, the fracture of the mortar results essentially from the (horizontal) spalling of the sand grains in few locations. The cracks in the cement paste and the spalling of sand grains link to lead to the global fracture of the mortar.

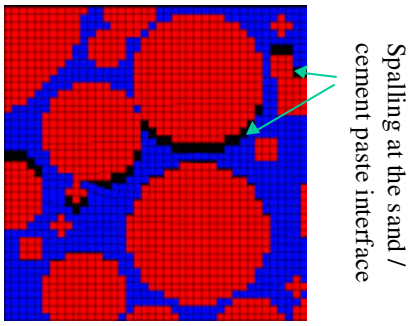

Figure 9. Deformed mesh of the specimen in tension.

The damage field in the *x*-direction is displayed in Figure 10 for the compression test (there is no significant damage in the *y*-direction).

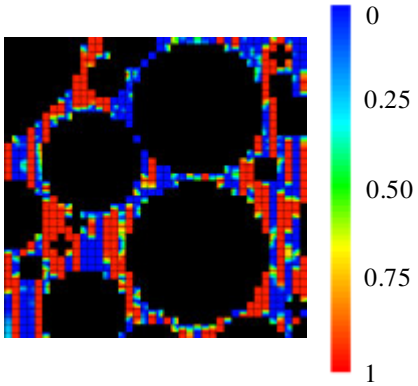

Figure 10. Damage field (D_x variable) for the compression test.

The deformation of the specimen is presented in Figure 11.

In the compressive test, the results are different from the tensile one. The cracks are essentially vertical (damage variable D_x). They are located at many different locations (and not localized as in the tension test). Furthermore, a (vertical) spalling of the sand grains is observed at many locations (unlike the tension test).

These results are similar to the ones observed experimentally in tension/compression tests and to the ones obtained numerically by Schorn (1992), Tijssens et al. (2001) and Cianco et al. (2003).

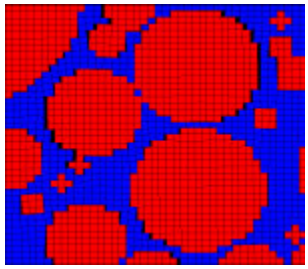

Figure 11. Deformed mesh of the specimen in compression.

3.2 *Drying shrinkage simulations*

Drying shrinkage simulations are then performed on a mortar which is constituted of 35 % of sand and 65 % cement paste. The specimen is a 2-cm-side square. The digital meso-structure used for the numerical simulation is given in Figure 12.

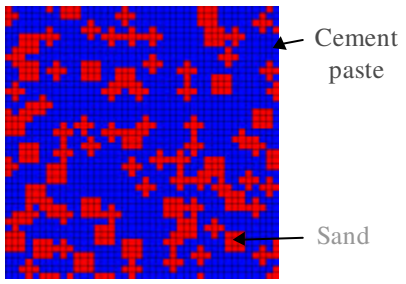

Figure 12. Digital picture of the mortar.

At the top face, the specimen is submitted to a relative humidity equal to 30 %. All the other sides are protected from desiccation. The other boundary conditions are given in Figure 13.

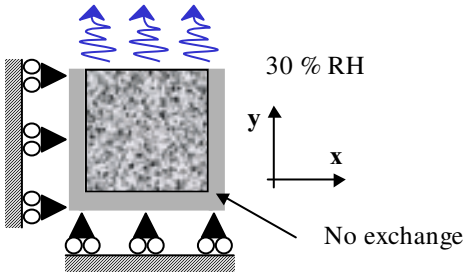

Figure 13. Illustration of the boundary conditions for the numerical simulations during the drying test.

The water content field is given in Figure 14 after 28 days of drying. It should be noted that the value of 128 $l.m^{-3}$ corresponds to the saturation.

Drying process occurs only in the cement paste. Therefore, sand grains act as obstacles for the diffusion of water. The drying process does not develop as a vertical progression of a diffusion front. There is a gradient of water content (and relative humidity) both in the *x* and *y*-directions.

The damage fields in *x* and *y*-directions are displayed in Figure 15.

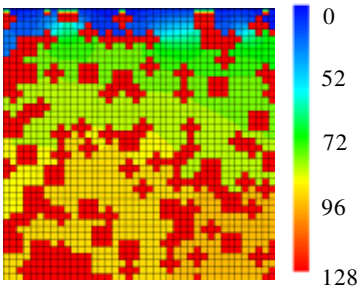

Figure 14. Water content field after 28 days of drying.

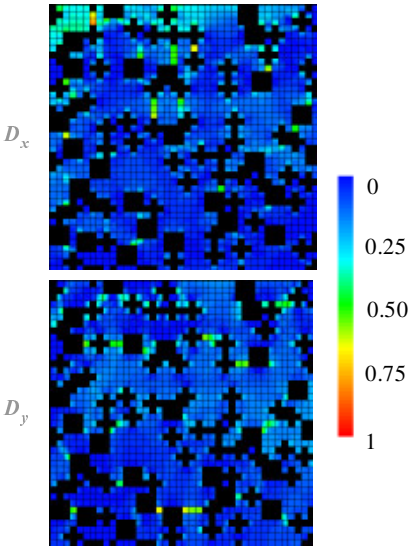

Figure 15. Damage fields (D_x and D_y variables) for the drying shrinkage test.

When the drying process occurs only in one direction as in a homogeneous material (for instance in the *y*-direction), cracks are preferentially oriented in the direction perpendicular to the drying one (for instance in the *x*-direction) and localized in the skin. Indeed, cracking occurs due to the fact that inner parts of the material shrink much slower than the skin.

In the case of a heterogeneous material, as in the studied mortar, cracking occurs both in the *x* and *y*-directions (Fig. 15). There are two main reasons. Firstly, a gradient of water content occurs in all the directions, which leads to differential shrinkage. Finally, sand grains strain is not affected by drying, while the cement paste shrinks in an isotropic manner. Therefore, the restraint effect of sand grains leads to an additional damage in the cement paste (with respect to one induced by differential shrinkage in the cement paste).

These results have been observed experimentally on mortars made of cement paste and glass spheres (with mechanical parameters similar to the sand ones), by Bisshop & van Mier (2002).

4 CONCLUSIONS

The effects of sand grains on the behavior of mortars have been numerically studied for mechanical and drying loadings. A mesoscale model has been used, in which cement paste, sand grains and ITZ have been considered. It is based on a poro-mechanical modeling, where shrinkage, creep and cracking have been associated in a physical manner, which is quite innovative.

Numerical simulations on a digital structure of a mortar retrieve many experimental observations. They show that in tension, a single crack through the ITZ (spalling of the sand grains.) and the cement paste leads to the failure of the material. In compression, the cracks are perpendicular to the direction of the loading and distributed more homogenously in the cement paste. Moreover, many spallings of the sand grains are noticed.

During drying, shrinkage microcracking is not only due to the self-equilibrated stresses in the cement paste (self-restraint due to non-uniform shrinkage strain). Numerical simulations show that microcracking is also due to the restraint effect of sand grains, which prevent the cement paste to deform. Moreover, they highlight that the generated microcracking is not preferentially oriented: microcracking is more isotropic than in the case of a homogeneous material (Benboudjema 2002). These results are consistent with the ones observed experimentally (Bisshop and van Mier 2002). To the authors' knowledge, such numerical observations have not been obtained yet.

Further numerical simulations have to be performed in order to investigate the effects of aggregates and ITZ in the behavior of mortar or concrete. The effects of size, shape, particle size distribution, concentration and mechanical properties of aggregate, as well as the influence of ITZ properties, need to be studied. Moreover, all the numerical simulations were made on a virgin specimen, although early-age cracking occurs probably at the cement paste/aggregate interface.

Hence, the study of early-age behavior of concrete (including endogenous and thermal shrinkage) will allow for knowing the initial state of the material. Finally, the study of basic and drying creep can bring additional information on the behavior of concrete. These task are currently under investigations.

5 REFERENCES

Bažant, Z.P. 1976. Instability, ductility and size effect in strain softening concrete. *Journal of Engineering Mechanics* 102: 331-344.

Bažant, Z. P. 2001. Prediction of concrete creep and shrinkage: past, present and future. *Nuclear Engineering Design* 203: 27-38.

Benboudjema, F. & Meftah, F. & Torrenti, J.-M., Sellier, A. & Heinfling, G. 2001. A basic creep model for concrete subjected to multiaxial loads. *4th International Conference on Fracture Mechanics of Concrete and Concrete Structures*; *Proc. intern. symp*, *Cachan, 28-31 Mai 2001,*. Balkema.

Benboudjema F. 2002. Modélisation des déformations différées du béton sous sollicitations biaxiales. Application aux enceintes de confinement de bâtiments réacteurs des centrales nucléaires, *PhD Thesis*, *Université de Marne-La-Vallée*. http://farid.benboudjema.free.fr (in french)

Bentz, D.P. 1997. Three-dimensional simulation of Portland hydration and microstructure development, *Journal of the American Ceramic Society* 80(1):3-21.

Bisshop, J. & van Mier, J.G.M. 2002. Effect of aggregates on drying shrinkage microcracking in cement-based composites. *Materials and Structures* 35: 453-461.

Ciancio, D. & Lopez, C.M. & Carol, I. & Cuomo, M. 2003. New results in mesomechanical modelling of concrete using fracture-based zero-thickness interface elements. *Computational Modelling of Concrete Structures*; *Proc. intern. symp., St. Johann im Pongau, 17-20 March 2003*. Balkema.

Feenstra, P.H. 1993. Computational aspects of biaxial stress in plain and reinforced concrete, *PhD thesis, Delft institute of technology*. Netherlands.

Goltermann, P. 1995. Mechanical predictions of concrete deterioration – Part 2: classification of crack patterns. *ACI Materials Journals* 92(1): 58-63.

Granger, L.P. & Bažant, Z.P. 1995. Effect of composition on basic creep of concrete and cement paste, *Journal of Engineering Mechanics* 121(11): 1261-1270.

Hillerborg, A. & Modeer, M. & Petersson, P.E. 1976. Analysis of crack formation and crack growth in concrete by means of fracture mechanics and finite elements. *Cement and Concrete Research* 6(6): 773-782.

Katz, A. & Bentur, A. & Kjellsen, K.O. 1999. Normal and high strength concretes with lightweight aggregates. In M.G. Alexander & G. Arliguie & G. Ballivy & A. Bentur & J. Marchand (eds), *Engineering and Transport Properties of the Interfacial Transition Zone in Cementitious Composites*: 71-88. RILEM Report 20.

Kim, J.K. & Lee, C.S. 1998. Prediction of differential drying shrinkage in concrete. *Cement and Concrete Research* 28 (7): 985-994.

Lee, J. & Fenves, G.L. 1998. Plastic-damage model for cyclic loading of concrete structures. *Journal of Engineering Mechanics* 124 (8): 892-900.

Li, G. & Zhao, Y. & Pang, S.-S. & Li, Y. 1999. Effective Young's modulus estimation of concrete. *Cement and Concrete Research* 29: 1455-1462.

Nielsen, A.U. & Monteiro, P.J.M. 1993. Concrete: A three phase material. *Cement and Concrete Research* 23: 147-151.

Nielsen, A.U. & Monteiro, P.J.M. & Gjorv, O.E. 1993. Estimation of the elastic moduli of lightweight aggregate. *Cement and Concrete Research* 25: 276-280.

Roelfstra, P.E. & Sadouki, H. & Witmann, H. 1985. Le béton numérique. *Materials and Structures* 18: 309-317.

Schorn, H. 1992. Numerical simulation of altering mechanical properties of concrete due to material behavior of the interfaces. In J.C. Maso (ed.), *RILEM International Conference Interfaces in Cementitious Composites; Proc. intern. symp.,* Toulouse, 21-23 October 1992. RILEM.

Sengul, O. & Tasdemir, C. & Tasdemir, M.A. 2002. Influence of aggregate type on mechanical behaviour of normal and high-strength concretes. *ACI Material Journal* 99(6): 528-533.

Soroka, I. 1979. *Portland cement paste and concrete*. London, Macmillan.

Tijssens, M.G.A. & Sluys, L.J. & van der Giessen, E. 2001. Simulation of fracture of cementitious composites with explicit modelling of microstructural features. *Engineering Fracture Mechanics* 68: 1245-1263.

van Mier, J.G.M. 1991 Mode I fracture of concrete: discontinuous crack growth and crack interface gain bridging. *Cement Concrete Research* 21: 1-15.

van Mier J.G.M., Vervuurt A. 1999. Test methods and modelling for determining the mechanical properties of the ITZ in concrete. In M.G. Alexander & G. Arliguie & G. Ballivy & A. Bentur & J. Marchand (eds), *Engineering and Transport Properties of the Interfacial Transition Zone in Cementitious Composites*: 19-52. RILEM Report 20.

Wittmann, F.H. & Roelfstra P. 1980. Total deformation of loaded drying creep. *Cement and Concrete Research* 10: 601-610.

Xi, Y. & Bažant, Z.P. & Jennings, H. & M. 1994. Moisture diffusion in cementitious materials - adsorption isotherms. *Advanced Cement Based Materials* 1: 258-266.